THE JOURNAL OF PHYSICAL CHEMISTRY C

Feature Article

pubs.acs.org/JPCC

Photoelectrochemical Tandem Cells for Solar Water Splitting

Mathieu S. Prévot and Kevin Sivula*

Laboratory for Molecular Engineering of Optoelectronic Nanostructures, Institute of Chemical Sciences and Engineering, École Polytechnique Fédérale de Lausanne, Station 6, 1015 Lausanne, Switzerland

ABSTRACT: In order to be economically competitive with simple "brute force" (i.e., PV + electrolyzer) strategies or the production of promising solar fuels, like H_2, from fossil fuels, a practical photoelectrochemical device must optimize cost, longevity, and performance. A promising approach that meets these requirements is the combination of stable and inexpensive oxide semiconductor electrodes in a tandem photoelectrochemical device. In this article, we give an overview of the field including an examination of the potential solar-to-fuel conversion efficiency expected in a device with realistic losses. We next discuss recent advances with increasing the performance of promising semiconductor electrode materials and highlight how these advances have led to state-of-the-art solar-to-chemical efficiencies in the 2−3% range in real devices. Challenges for further optimization are further outlined.

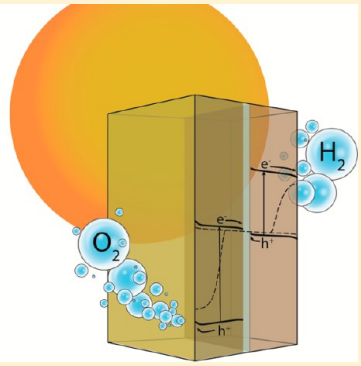

1. INTRODUCTION

The realization of a sustainable energy economy is contingent on developing an energy vector that can be efficiently (re)generated from renewable sources, easily stored, and straightforwardly transported to the point of use. Chemical fuels, which store energy in covalent bonds, are especially attractive for this purpose, as the infrastructure for the widespread use of fossil fuels is already in place. Solar fuels produced by photon-to-chemical energy conversion are promising substances to fulfill this need. In particular, producing H_2 from another renewable resource, water, using only sunlight as input energy has been thought of as an attractive goal for decades. Indeed, solar hydrogen is considered the central element in a multifaceted and interconnected chemical network—a "solar refinery"—which will ultimately convert photons from the sun into raw materials for industrial synthesis and carbon-based chemical fuels.[1] The overall electrochemical reaction of water splitting consists of both reduction and oxidation half-reactions as follows (with reaction potentials against the reversible hydrogen electrode, RHE):

Reduction reaction:

$$2H^+ + 2e^- \rightarrow H_2 \quad (E^0_{red} = 0.00\ \text{V vs RHE})$$

Oxidation reaction:

$$2H_2O + 4h^+ \rightarrow O_2 + 4H^+ \quad (E^0_{ox} = -1.23\ \text{V vs RHE})$$

Overall reaction:

$$2H_2O \rightarrow 2H_2 + O_2 \quad (\Delta E = -1.23\ \text{V})$$

Since the overall reaction has a negative standard potential energy must be added for water splitting to occur. We need only to consider how to use solar energy to supply the energy need to drive this reaction. While this possibility seems straightforward, special attention is needed if this scheme is to be considered as a viable route for converting solar energy on a scale commensurate with the global energy demand. For instance, any system for converting solar energy must find a balance between minimizing system complexity (i.e., device cost) and maximizing device performance (i.e., energy conversion efficiency and device longevity) given the relatively low energy density of solar irradiation. Moreover, any economically feasible system for solar hydrogen production must also compete with the price of H_2 generated from conventional sources (US$ 2−3 kg^{-1} for the steam reforming of natural gas).[2]

Traditionally, the electrical potential required to drive the overall water splitting reaction can be supplied by any direct current (DC) source to an electrolyzer, where the reduction reaction takes place at the cathode and the oxidation reaction takes place at the anode. While a difference in bias of only 1.23 V should be sufficient to split water into H_2 and O_2, due to the entropic increase needed to drive this process as well as the overpotential required to overcome kinetics of the oxygen and hydrogen evolution reactions, modern alkaline electrolyzers usually operate at voltages above 1.8 V.[3] The most obvious approach to generate sufficient voltage for water splitting with solar energy is to connect multiple standard photovoltaic (PV) cells in series. For example, a traditional pn-junction silicon PV produces a potential of 0.5−0.6 V at its maximum power point under standard conditions. Thus, three or four of these connected electrically in series would create sufficient potential to split water (depending on the type of electrolyzer employed). This "brute force" PV + electrolysis approach is limited by the price and availability of PV devices and electrolyzers, and currently results in a price of H_2 produced

Received: May 29, 2013
Revised: July 11, 2013
Published: July 26, 2013

   dx.doi.org/10.1021/jp405291g | J. Phys. Chem. C 2013, 117, 17879−17893

around US$10 kg^{-1} assuming an installed cost of $2 per peak watt[4] (which is the expected target for installed residential PV by the year 2020 according to the US DOE SunShot initiative[5]). While this price can certainly decrease as the PV market grows, a major and general drawback comes from the voltage output of a tradition pn-junction solar cell, which is strongly dependent on the illumination intensity. This implies that the optimum number of cells required to generate sufficient potential is highly variable due to variations in light intensity caused by haze, cloud cover, or time of day. This important disadvantage can result inasmuch as a 50% energy loss, and challenges the viability of the PV + electrolysis approach. Then again, this has also inspired researchers to develop systems that can potentially avoid this drawback and also convert solar energy at a price competitive with fossil sources. Developing systems that meet these goals remains a major challenge, but the severity of the global energy situation has stimulated the development of many promising routes. In this feature, we describe progress toward developing an inexpensive device for the direct conversion of solar energy into hydrogen fuel using a photoelectrochemical tandem cell.

2. DIRECT SOLAR WATER SPLITTING WITH PHOTOELECTROCHEMICAL CELLS

Compared to the PV + electrolysis approach, a more straightforward path to light-driven chemical transformations is to directly interface a semiconductor and the electrolyte as in a photoelectrochemical (PEC) device. Not only does this route eliminate the need for a separate electrolyzer (reducing system complexity), fewer electron transfer steps are also required, reducing the number of potential loss channels in the system. When a semiconductor is placed in direct contact with an electrolyte, the equilibration of the semiconductor's chemical potential (the Fermi level) with the oxidation/reduction potential of the electrolyte can generate an electric (space-charge) field in the semiconductor of width W, at the semiconductor–liquid junction (SCLJ). Upon the absorption of a solar photon with energy $h\nu > E_g$ (the semiconductor band gap energy), this space-charge field can separate photo-generated electrons in the semiconductor's conduction band from their corresponding holes in the valence band. In contrast to a traditional photovoltaic cell where the photogenerated charge carriers are extracted by electrical contacts into an electric circuit, excited charge carriers in a PEC electrode travel to the SCLJ to perform redox chemistry directly. For example, with an n-type photoanode under illumination, photogenerated holes directly oxidize water into O_2, while, for a p-type photocathode, photogenerated electrons can directly reduce water into H_2. In either case, the single photoelectrode absorbs two photons to produce one molecule of H_2 (the so-called S2 approach), and must generate sufficient external chemical potential (free energy, $\Delta\mu_{ex}$) with these photons to overcome the 1.23 V required to split water plus the electrochemical overpotentials for the oxidation and reduction reactions, η_{ox} and η_{red}, respectively.

Historically, interest in performing inexpensive solar water splitting using a PEC device goes back decades, and was first demonstrated using TiO_2 as a single semiconductor absorber in an S2 approach over 40 years ago.[6] As an oxide semiconductor, TiO_2 offers excellent stability in the relatively harsh aqueous conditions of water splitting. However, this material possesses a semiconductor band gap energy, E_g, around 3.2 eV. Thus, it cannot harvest a significant portion of the solar spectrum and therefore its potential solar-to-hydrogen conversion efficiency is very low (less than 2%). Because of this, following the demonstration with TiO_2, substantial effort was invested toward developing ideal PEC materials. To date, the challenge of identifying a single semiconducting material that can offer substantial solar light harvesting, adequate stability in the harsh aqueous electrolytes required, and appropriate conduction and valence band energy levels straddling the water reduction and oxidation potentials has proven very difficult. However, since the water splitting reaction inescapably requires two separate half-reactions, it seems obvious to use two light absorbers for PEC water splitting.

Indeed, a simple two-photoelectrode approach to construct a PEC water splitting cell is to use an n-type semiconductor photoanode together with a p-type semiconductor cathode. The electrochemical energy scheme for this type of device in a "wireless" configuration is shown in Figure 1 for a photoanode/

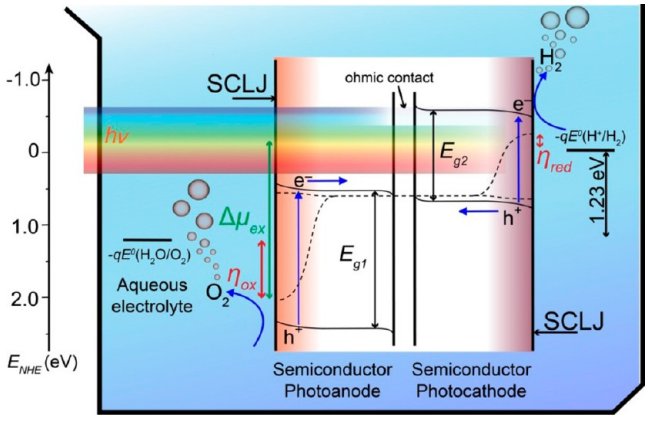

Figure 1. Electron energy scheme of PEC water splitting using a dual-absorber tandem cell. The absorption of a photon ($h\nu$) by a semiconductor with a band gap (E_g) creates an electron–hole pair that can be separated by the space charge layer to generate a photopotential (as indicated by the splitting of the Fermi level, broken line). The combination of two absorbers as shown will increase the free energy ($\Delta\mu_{ex}$) available. This free energy must be greater than the energy needed for water splitting (1.23 eV) plus the overpotential losses at both the anode and the cathode, η_{ox} and η_{red}, for the water splitting reaction to occur. Four photons must be absorbed in this mechanism to produce one molecule of H_2.

photocathode type tandem cell with band gap energies E_{g1} an E_{g2}, respectively, and assuming $E_{g1} > E_{g2}$. In this approach with two photoelectrodes where each absorbed photon creates one excited electron–hole pair, four photons (two in each absorber) must be absorbed to create one molecule of H_2 (called a D4 approach, accordingly). In addition, to optimize solar photon harvesting, the cells can be placed one on top of the other (i.e., in tandem) and photons not absorbed by the first cell are transmitted to and absorbed by the second. To motivate the development of this type of device, Weber and Dignam[7] evaluated the potential solar to hydrogen conversion efficiency, η_{STH}, of this tandem approach compared to simply placing two cells of the same band gap energy side by side. While the evaluation of the side-by-side approach gave an upper limit of 16.6% with $E_{g1} = E_{g2} = 1.4$ eV (a moderate increase over the 11.6% predicted with a single absorber approach), using the integrated tandem approach, 22% η_{STH} was predicted to be possible with $E_{g1} = 1.8$ eV and $E_{g2} = 1.15$ eV. Since it is important to know a reasonable value for the maximum

dx.doi.org/10.1021/jp405291g | J. Phys. Chem. C 2013, 117, 17879–17893

expected solar energy conversion with reasonably foreseen losses in a real system, a more extensive analysis by Bolton plotted the maximum η_{STH} with respect to different absorber band-gaps and realistic losses.[8,9] In this work, it was assumed that each semiconductor absorbs all photons with energy $h\nu > E_g$ and transmits all photons with energy $h\nu < E_g$. No reflection or scattering losses were included. Following the method of Bolton, if a minimum reasonable value for the energy loss, $U_{loss} = E_{g1} + E_{g2} - \Delta\mu_{ex} + \eta_{ox} + \eta_{red}$, is chosen to be 2.0 eV (or 1.0 eV for each semiconductor), the maximum expected η_{STH} as a function of the chosen band gap energies, E_{g1} and E_{g2}, can be predicted considering the distribution of photons in standard solar illumination (AM 1.5G 1000 W m^{-2}). Figure 2a shows a

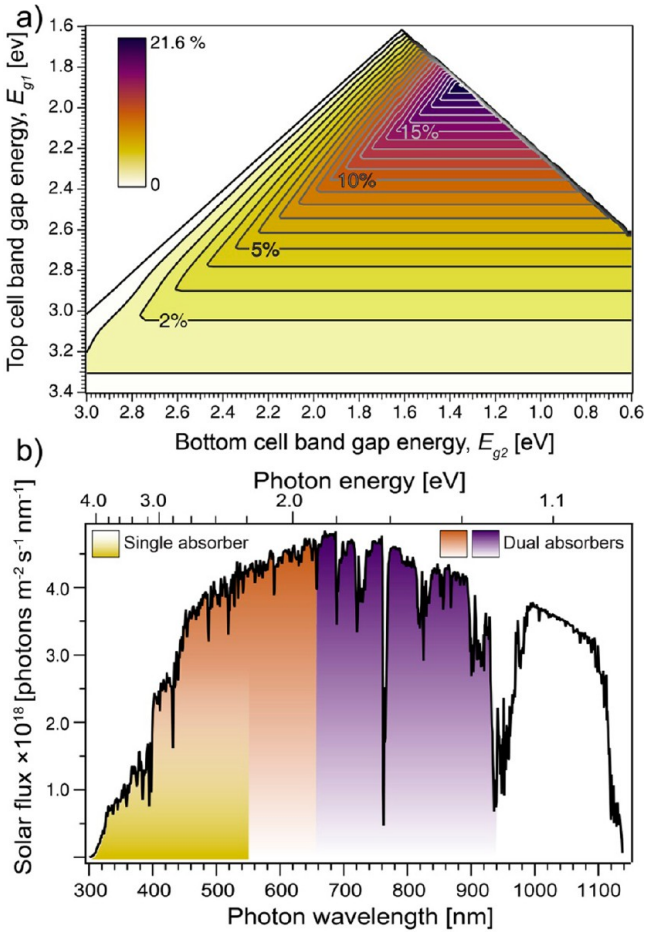

Figure 2. (a) Contour plot (thick gray lines) showing the maximum predicted η_{STH} with AM 1.5G incident radiation (1000 W m^{-2}) and a total loss, U_{loss}, set at 2.0 eV as it depends on the chosen semiconductor band gap energies, $E_{g,i}$, i = 1, 2 (with $E_{g1} > E_{g2}$). (b) The benefits of the tandem cell approach are shown through the AM 1.5G solar photon flux as a function of wavelength and photon energy. The shaded area of the spectrum represents the photos that could be harvested using a single semiconductor absorber (yellow) and a dual absorber tandem approach (light brown and purple).

contour plot of this case based on Bolton's method using the ASTM G173-03 Reference Spectra[10] and further assuming that the two semiconductors are connected in series (so that the photocurrent density must be equal).

The shapes of the contours (gray lines), which represent values of E_{g1} and E_{g2} that result in the same η_{STH}, are easily rationalized. First, no contours are present in the upper left of the plot, as this is where the set condition $E_{g1} > E_{g2}$ is not satisfied. The upper right region, where η_{STH} is also not defined, represents semiconductor combinations that do not possess sufficient $\Delta\mu_{ex}$ for water splitting in a dual absorber configuration given the assumed U_{loss}. The contours also have a shape defined by an abrupt change in direction (e.g., where E_{g1} = 2.69 eV and E_{g2} = 2.34 eV on the 5% contour) where the device limiting the photocurrent switches, indicating that each absorber is producing the maximum possible amount of photocurrent at the turning point. The boundary defined by these "current matching" points divides a region to the lower left (where the predicted efficiency is limited by the light absorption of the top cell) from the upper right (where η_{STH} is limited by the bottom cell).

Remarkably, even with the large assumed losses in the tandem cell, a maximum η_{STH} of 21.6% is predicted using optimum values of E_{g1} = 1.89 and E_{g2} = 1.34 eV. This is a significant improvement over the single absorber case, which is predicted to give only η_{STH} of 12.7% under optimum conditions (using E_g = 2.23 eV) with the same assumed losses (1.0 eV per photon). The photon harvesting of the standard solar spectra using the optimized tandem cell compared to the single absorber approach is shown in Figure 2b. Here, the advantage of the tandem cell can be clearly seen as the top cell harvests more of the spectra compared to the single absorber approach.

In addition to our revision of Weber and Dignam's classic analysis above with large losses, we note that, during the preparation of this work, Lewis and co-workers published detailed balance calculations that account for the Shockley–Queisser limit on the $\Delta\mu_{ex}$ of each absorber.[11] The maximum STH efficiency for a water splitting photoanode/photocathode tandem cell was found to be 29.7% with E_{g1} = 1.60 and E_{g2} = 0.95 eV. Thus, while the conditions and losses specified in a model can lead to a varied maximum predicted η_{STH}, it is clear that a quite attractive solar-to-hydrogen conversion efficiency (at least) over 20% and possibly even up to 30% can be expected with a tandem PEC cell. However, the optimum band gap energy range for these maximum efficiencies is narrow, and presents a significant challenge for materials development. Then again, considering that standard single crystal silicon PV modules coupled to high-pressure electrolysis give only up to about 9.3%,[12] a PEC tandem cell with over 10% η_{STH} is a reasonable goal, and this relaxed constraint leaves a wide window of suitable E_g's to choose from. Of course, achieving this still depends on identifying materials with the correct band gap energies and band positions suitable for the water oxidation and reduction reactions. Notably, this has been accomplished using monolithic, epitaxially grown III–V semiconductor systems and high-performance PEC tandem cells have been demonstrated with impressive η_{STH} up to 12.5%.[13] However, the $GaInP_2$ photocathode used quickly corrodes when in contact with the aqueous electrolyte.[14] Indeed, realizing a practical device further requires that the materials employed are widely available, inexpensive to prepare, and stable in a water splitting PEC cell. This goal has been the focus of our research at EPFL as well as many other groups.

3. OXIDE SEMICONDUCTORS AS PHOTOANODES

While many n-type photoanodes have been considered for the water oxidation half-reaction, identifying a material that remains stable in the harsh conditions of water oxidation has proved to be quite difficult. Transition metal oxide semiconductors have, however, excelled in this aspect, with the prototype being

dx.doi.org/10.1021/jp405291g | J. Phys. Chem. C 2013, 117, 17879–17893

TiO_2.[6,15] Moreover, solution-based processes like sol−gel, spray pyrolysis, or hydrothermal routes can be easily used followed by thermal annealing to obtain oxide thin film electrodes without expensive processing techniques. For TiO_2, the rutile or anatase phases exhibit a band gap energy in the range 3.0−3.2 eV which unfortunately limits its potential solar-to-hydrogen conversion efficiency to around 2%, even if used in a current-matched tandem cell. However, due to its favorable aspects, stability, and activity for photoelectrochemical water oxidation, an intense amount of effort has been focused on increasing the light absorption of TiO_2 with research reports appearing as early as 1977.[16] However, the lack of success in increasing the energy conversion efficiency of TiO_2 using sunlight to above ∼1% over the last ∼30 years has resulted in skepticism concerning the potential with this approach.[17] Despite this, interest remains and some recent reports have renewed promise. For example, Chen et al. suggested a potentially successful route to enhancing the light absorption by using hydrogenated anatase TiO_2 nanocrystals and tuning the amount of lattice disorders.[18] In this way, midgap electronic states were created, accompanied by a reduced band gap. The resulting black TiO_2 nanocrystals exhibited substantial activity and stability (over 22 days) in the photocatalytic production of hydrogen from water under sunlight. Another modern strategy to increase light absorption on TiO_2 has been to harness plasmonic resonance.[19−21] In one report, Cronin and co-workers prepared TiO_2 photoanodes with integrated Au nanoparticles and demonstrated a 66-fold increase in photocurrent using photons with energy 1.96 eV (well below the band gap energy of TiO_2).[21] In general, commercializing plasmonically enhanced electrodes becomes more interesting with the possibility to employ non-noble metals to reduce electrode cost.[22]

A perhaps simpler alternative to searching for a method to increase the light absorption of TiO_2 is to employ a different stable oxide with a smaller band gap energy. Generally, the band gap energy of a transition metal oxide is defined by oxygen 2p states on the valence band and metal d orbitals for the conduction band. An oxide with a smaller band gap energy will thus most probably have a similar valence band but a conduction band at a lower energy. This is in fact ideal for the use of transition metal oxides as photoanodes in tandem cells, and while there are numerous binary and hundreds of possible ternary transition metal oxides, relatively few have been identified as suitable for the water oxidation reaction. These few notable examples like WO_3,[23] $BiVO_4$,[24] and Fe_2O_3[25] have been well-developed by a number of groups. The maximum possible solar-to-hydrogen conversion efficiency as a function of the oxide band gap energy, assuming it is used as a top cell and the same reasonable losses are present that were used for Figure 2, is shown in Figure 3. Typically, research on these oxide materials has focused on increasing the photocurrent density (in units of mA cm^{-2}) measured with respect to an applied potential (reported versus a known reference) under standard solar illumination. This photocurrent is a good metric of the number of photogenerated charge carriers that reach the SCLJ and participate in an oxidation reaction. As long as the Faradaic efficiency of water oxidation is unity,[26] the photocurrent corresponds directly to the rate of water splitting. The maximum photocurrent possible for a photoanode under standard conditions is also shown in Figure 3.

As the original low-band gap oxide alternative to titanium dioxide, tungsten trioxide was first reported shortly after the initial demonstration with TiO_2.[27] With a band gap energy of

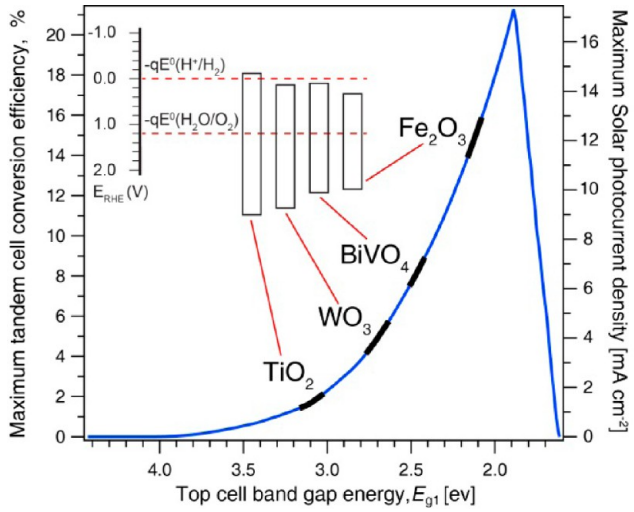

Figure 3. Maximum solar-to-hydrogen conversion efficiency and solar photocurrent as a function of the top cell band gap energy in a tandem cell with the loss assumptions identical to Figure 2. The band gap energies and efficiency range for commonly used semiconductor oxide photoanodes are also shown.

2.6−2.8 eV, it could be the top absorber in a tandem cell that could potentially convert up to about 6% of the standard sunlight into hydrogen. In the past decade, Augustynski and others have optimized the solution-based preparation of nanostructured thin film electrodes of electrodes of WO_3 that achieve incident photon-to-electric current efficiency (IPCE) of up to 90% and solar photocurrents in the 2−3 mA cm^{-2} range with the application of an external bias (customarily reported at the water oxidation potential, 1.23 V vs RHE).[28] Similar to TiO_2, more recent efforts with this material have focused on increasing its photon harvesting ability. For example, a small amount of additional photocurrent can also be extracted using a plasmonic approach,[29] and doping has been extensively investigated.[30] However, while WO_3 remains an important model compound, the high IPCE values already reported suggest that the return on further optimization of this material is limited.

Bismuth vanadate is a comparatively more recent material exploited as a photoanode. The monoclinic scheelite phase of $BiVO_4$, with a band gap of about 2.4 eV, was shown to be photoactive for water oxidation in 1999.[31] From Figure 3, this material could reach solar-to-hydrogen efficiencies of over 9% in a tandem cell when used with a second absorber of E_g < 1.9 eV. Over the past decade, rapid development has shown improvements of the photocurrent of $BiVO_4$ based photoanodes resulting mostly from the incorporation of substitutional dopants like W[32,33] and Mo[34] to increase the majority carrier transport. Water oxidation photocurrents have been observed up to 2.8 mA cm^{-2} under standard conditions using Mo as a dopant.[35] One drawback exhibited by this material has been the large overpotential required to drive the oxygen evolution reaction (OER). To overcome this, OER catalysts like RhO_2[35] and cobalt-phosphate (Co-Pi)[36−38] have been applied to give a remarkable reduction of overpotential and reasonable photocurrent (over 1 mA cm^{-2} under AM 1.5G illumination) at potentials under 1.23 V vs RHE. This is shown in Figure 4 with the Co-Pi catalyst where the authors also compare the photocurrent with a one-electron sacrificial probe (H_2O_2[39]) to demonstrate that the Co-Pi/$BiVO_4$ electrode

dx.doi.org/10.1021/jp405291g | J. Phys. Chem. C 2013, 117, 17879−17893

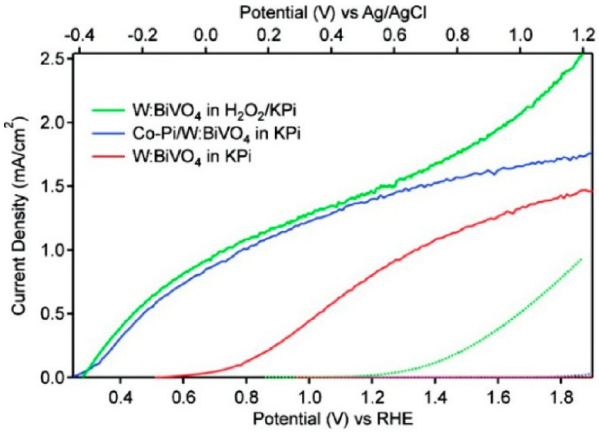

Figure 4. *J*–*V* curves measured for a W:$BiVO_4$ photoanode in 0.1 M KPi buffer (pH 8) under 1 sun AM 1.5 front-side illumination (solid) and in the dark (dotted). The red curve describes PEC water oxidation by the W:$BiVO_4$ photoanode, and the green curve describes the PEC behavior after addition of 0.1 M H_2O_2 to the electrolyte solution. The blue curve describes PEC water oxidation by the W:$BiVO_4$ photoanode after Co-Pi deposition. Reprinted from ref 37.

almost completely eliminates losses due to electron–hole recombination at the SCLJ (but recombination in the bulk remains).[37] Overall, the relatively low IPCEs observed with this material (<50%) suggest that further research could push photocurrents over the 5 mA cm^{-2} benchmark under standard conditions if the bulk recombination can be reduced.

Hematite (α-Fe_2O_3) is also a promising transition metal oxide with a band gap of ca. 2.1 eV. This corresponds to a maximum η_{STH} of ca. 15% according to Figure 3, if a second absorber with E_{g2} < 1.5 eV is used. Besides its relatively small band gap, α-Fe_2O_3 is the most stable form of iron oxide under ambient conditions, and since iron is ubiquitous in the earth's upper crust, hematite is an outstanding candidate for solar energy conversion on a scale commensurate with the global energy demand. Hardee and Bard[40] first turned to Fe_2O_3 as a material for water photolysis in 1976 seeking a photoanode material that was both stable under anodic polarization and capable of absorbing light with wavelengths longer than 400 nm. Over the next decade, numerous reports were published describing continuing studies with pure and doped Fe_2O_3 made by various routes. Noteworthy photoelectrochemical studies were performed on Ti doped polycrystalline sintered hematite pellets[41,42] and Nb doped single crystals,[43] which led to IPCEs up to about 40% at 370 nm and 1.23 V vs RHE in 1 M NaOH. However, the first decade of work identified the many challenges of employing this material for photoelectrochemical water splitting, most notably a large overpotential and slow water oxidation kinetics,[42] a low absorption coefficient, requiring relatively thick films,[44,45] poor majority carrier conductivity,[43,46] and a short diffusion length of minority carriers.[41] These limitations suggested that a compact thin film geometry was not suitable for hematite, and indeed, modern reports with hematite have shown that photocurrents can be drastically increased by careful nanostructuring. A review of this work has been recently published.[25] At EPFL, we have demonstrated solar photocurrents in excess of 3.0 mA cm^{-2} at 1.23 V vs RHE with nanostructured films prepared using atmospheric pressure chemical vapor deposition (APCVD) and coated with an OER catalyst (IrO_2),[47] and comparable photocurrents have been achieved with a solution-based colloidal approach.[48,49]

Given the poor charge carrier conductivity of Fe_2O_3, one approach that has gained recent success is the extremely thin absorber (ETA) or host–guest approach. We have first demonstrated this using nanostructured WO_3.[50] Here, a thin but conformal layer of the light absorbing iron oxide was coated on the oxide scaffold, eliminating the requirement of the Fe_2O_3 to transport charges long distances. More recently, photocurrents have been demonstrated over 1 mA cm^{-2} at 1.23 V vs RHE using atomic layer deposition with this approach on $TiSi_2$ "nanonets",[51] and 2.5 mA cm^{-2} at 1.4 V vs RHE using APCVD films on a high surface area conducting Nb:SnO_2 scaffold.[52] The drastic effect that the scaffold has on the photocurrent in this approach is shown in Figure 5. However, in general with

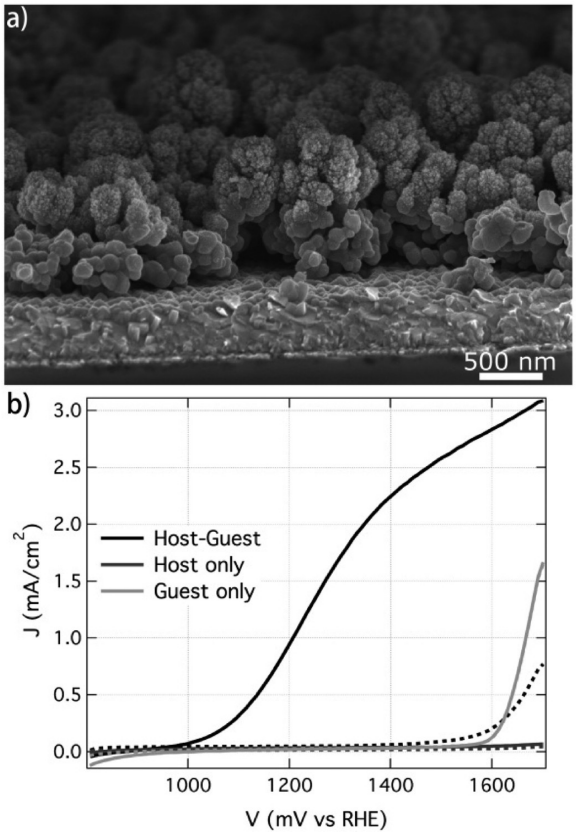

Figure 5. A "guest" material, hematite, deposited by APCVD into the Nb:SnO_2 host as evidenced by cross-sectional SEM (a). Current–voltage measurements under AM 1.5 simulated light in 1 M NaOH resulted in high photocurrents for the host–guest structure (black) and negligible photocurrents for the host-only and guest-only control samples (gray) (b). Dark currents are shown as dashed lines. Reprinted from ref 52.

this method, the increase in the interfacial area between the iron oxide and the scaffold has been shown to limit the photocurrent due to recombination.[53] This has instigated a line of research focused on engineering the interface between the iron oxide and the scaffold material.[54–56] SiOx,[56] SnO_2,[53] and Ga_2O_3[55] interfacial layers have been shown as promising buffers that decrease recombination. Most recently, Hisatomi et al. reported absorbed-photon-to-current efficiency (APCE) exceeding 40% under 400 nm illumination using films of Fe_2O_3 only 9 nm thick. This impressive APCE performance, which

dx.doi.org/10.1021/jp405291g | J. Phys. Chem. C 2013, 117, 17879–17893

rivals the best nanostructure thin films with optimized thickness over 500 nm, was enabled with a Nb_2O_5 underlayer deposited by ALD.[54] Further development of the ETA approach will no doubt lead to further increase in photocurrent with Fe_2O_3 based electrodes. For example, further development of ternary overlayers like the $ZnFe_2O_4$ employed by Choi and co-workers seems particularly promising.[57]

In addition to the morphology and interfacial recombination, other factors critical to the performance of hematite electrodes have been shown to be majority carrier transport and recombination at the SCLJ. The former issue is most typically addressed by substitutional cation doping,[58,59] and the latter issue was initially attributed to poor OER kinetics.[60] However, most recently, the role of recombination at surface trapping states has been recognized.[61] Surface passivation techniques using (non-OER promoting) overlayers like Al_2O_3[62] and In_2O_3[63] have been shown to eliminate some overpotential by reducing Fermi level pinning in these electrodes, and the subsequent addition of an OER catalyst can further reduce the overpotential.[64] Despite this, a large overpotential remains even in hematite electrodes with optimized surface treatments, and this has sparked debate over the nature of the role of the OER catalyst and the surface passsivating overlayers.[60,65] As will also be emphasized later on, the further reduction of the overpotential for water oxidation is of primary importance to hematite for its application in a water splitting device. Advancement on this front will make a large impact on the overall solar to hydrogen efficiency in real devices. In addition and in general for photoanode research, identifying stable oxide semiconductors with activity for the water oxidation reaction and a band gap energy around 1.9 eV is also a major goal in the field.[66]

4. PHOTOCATHODES AND PHOTOANODE/PHOTOCATHODE TANDEM CELLS

While numerous n-type semiconductors have been well-studied as photoanodes for water oxidation, comparatively very little work has been done on photocathodes for water reduction. To function as a photocathode, a semiconductor has to have a conduction band located cathodic of the water reduction potential and also exhibit p-type behavior, so, when it is immersed in water, minority carriers (electrons) are driven to the surface of the electrode at the SCLJ. In addition, it is necessary to find materials with a small enough band gap energy, so a significant portion of the visible light is harvested. Because the reductive side of the cell is not submitted to conditions as harsh as the ones present on the oxidative side (indeed, this electrode is cathodically protected against oxidation), the search for efficient photocathodes has not been limited to oxide materials. The very first photocathode for water splitting, reported by Yoneyama et al. in 1975, was a single crystal of p-type GaP, with a band gap of 2.38 eV.[67] Since this first report, many different semiconductors were suggested as photocathodes for water reduction. It is possible to group these materials in different categories: p-doped phosphides, p-doped chalcogenides, p-doped silicon, and p-doped oxides. Materials from these four categories have been suggested over the past decades, with increasing performances, in the search for low-cost and efficient photocathodes for water reduction.

Single-crystalline phosphides, such as p-GaP, p-InP, or p-$GaInP_2$, are good solar absorbers, with relatively low band gap energy, making them potential candidates for photoinduced water reduction. One of the first tandem PEC cells reported, with an n-$SrTiO_3$ photoanode and a p-GaP photocathode achieved, an overall 0.67% efficiency.[68] In 1982, Heller and co-workers reported that single-crystalline InP (E_g = 1.35 eV), once passivated by an oxide layer and coated with Rh or Re, achieved respectively 13.3 and 11.4% photocathodic conversion efficiencies in 1 M $HClO_4$.[69] Bockris and co-workers later reported 8.2% overall conversion efficiency for a PEC cell made of an n-GaAs photoanode and a single-crystalline p-InP photocathode.[70] $GaInP_2$ (E_g = 1.83 eV) has been studied by Turner and co-workers, and was shown to be reasonably stable under acidic conditions.[14] In 1998, they created a device made of a p−n GaAs photovoltaic junction connected with a crystalline p-$GaInP_2$ photocathode, and achieved a benchamrk 12.4% conversion efficiency in 3 M H_2SO_4.[13] However, despite high efficiencies, gallium and indium phosphides are not ideal for inexpensive large-scale production, due to the scarcity of their components and the need for them to be single-crystalline.

Chalcogenide p-type materials, initially developed for thin film photovoltaics, have also been explored as potential photocathodes for water reduction. Early studies showed that ZnTe (E_g = 2.25 eV) was unstable, whereas single-crystalline CdTe showed a relatively low band gap (E_g = 1.5 eV) and good stability at cathodic potentials under acidic conditions.[71] However, the expensive material achieved relatively low performances when used in combination with n-$SrTiO_3$: only 0.18% overall conversion efficiency (3.7 times lower than the p-GaP cathode). Finally, Zoski and co-workers reported a Pt-coated tungsten disulfide (p-WS_2, E_g = 1.3 eV) electrode with a cathodic conversion efficiency of 6−7% under 50 mW cm^{-2} (632.8 nm) light intensity, in 6 M H_2SO_4.[72] These early studies have served as an important foundation for the recent increase in interest in chalcogenides for photocathodes. For example, Lewis and co-workers very recently revisited p-WSe_2 and coated a crystalline (E_g = 1.2 eV) photocathode with platinum and ruthenium to achieve cathodic conversion efficiencies higher than 7%.[73] The authors also stressed the importance of the purity of the crystalline phase to achieve good minority-carrier diffusion lengths. $CuIn_{1-x}Ga_xSe_2$ (CIGS) is a modern and interesting chalcogenide because its band gap can be tuned between 1.0 and 1.7 eV, by modifying its Ga:In ratio. Domen and co-workers coated a p-CIGS electrode with a thin n-type CdS layer, and platinized it to produce a 12 mA cm^{-2} cathodic photocurrent at pH 9.5, although the light intensity was not specified.[74] The same group later successfully used the same approach with p-$CuGaSe_2$ (E_g = 1.65 eV),[75] a cheaper material initially reported by Miller and co-workers as suitable for photoinduced hydrogen production,[76] with photocurrent as high as 13 mA cm^{-2} in 0.5 M H_2SO_4 under 1 sun illumination. Finally, a recent report by Matsumura and co-workers showed that Pt-CdS-coated electrodes of p-$CuInS_2$ (p-CIS, E_g = 1.5 eV) and p-Cu(In,Ga)S_2 (p-Ga:CIS, E_g =1.5 eV), deposited by spray pyrolysis, were able to work as photocathodes for water reduction in 0.1 M europium nitrate.[77] Given these recent demonstrations, it is clear that several chalcogenide materials are very promising p-type semiconductors for water reduction. Requirements for small band gap and easy-to-process electrodes are met, and it should be possible to reach high efficiencies with cheap materials, based on abundant elements. While short-term stability studies seem promising with these materials, the long-term stability of these materials under operation remains an important issue for further development as well as replacing the n-type CdS overlayer used to promote charge extraction.

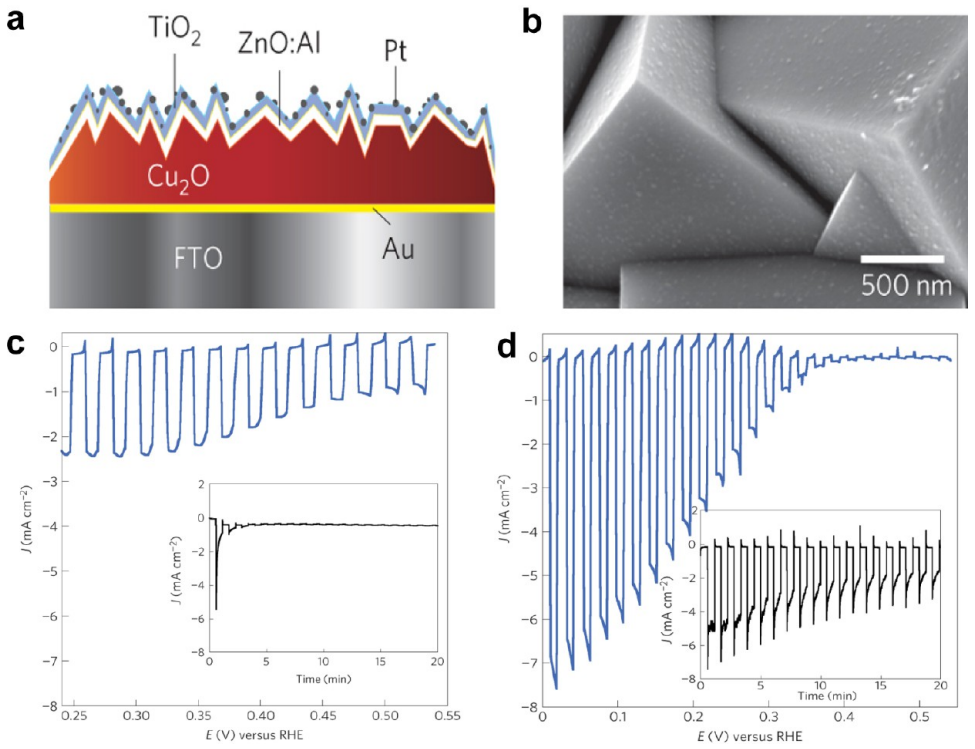

Figure 6. Top line: (a) Schematic representation of the Cu_2O electrode structure. (b) Scanning electron micrograph showing a top view of the electrode after ALD of ZnO:Al_2O_3 (20 nm)/TiO_2 (11 nm) followed by electrodeposition of Pt nanoparticles. Bottom line: Current–potential characteristics in 1 M Na_2SO_4 solution, under chopped AM 1.5 light illumination for the bare Cu_2O electrode (c) and for the as-deposited Cu_2O/ZnO:Al_2O_3 (20 nm)/11 nm TiO_2/Pt electrode (d). *E* is the electrochemical potential of the electrode. The insets show the respective photocurrent transients for the electrodes held at 0 V versus RHE in chopped light illumination with N_2 purging. Reprinted with permission from ref 92. Copyright 2011 Nature Publishing Group.

Because of its abundance and small band gap energy (1.12 eV), p-Si makes a good candidate for use in a tandem PEC cell. However, we note that, given the losses assumed for the efficiency prediction in Figure 2, a tandem cell will not generate sufficient $\Delta\mu_{ex}$ with a silicon photocathode unless a photoanode of $E_g > 2.2$ eV is used, limiting the conversion efficiency to ca. 15% at maximum. Even so, a lot of effort has been placed into improving the performances of silicon photocathodes since their first report in 1976.[78] An early study from Wrighton's group showed that, when functionalized with a bipyridinium compound and platinum acting as catalysts, a p-Si electrode achieved 5% efficiency when illuminated at 632.8 nm, as opposed to essentially no hydrogen generation for the bare material. However, the device showed poor stability, with a decrease of 20% in efficiency in the first hour.[79] In 1984, Tsubomura and co-workers reported increased efficiency, achieved by diffusing phosphorus into the material from its surface.[80] The resulting n^+p-Si material, when coated with platinum, showed 7.8% conversion efficiency in a 3 M HBr solution, oxidizing I^- from a HI solution at the anode. Again, the photocurrent was reported to decrease quickly, because of the formation of reduced species on the surface of the electrode. More recently, employing nanostructuring and morphology control techniques have led to important advances with Si photocathodes. For example, in 2011, Lewis and co-workers reported a microwire array of platinized n^+p-Si prepared by a templated vapor–liquid–solid growth process, which allowed the use of lower-purity Si compared to other deposition techniques.[81] Increased conversion efficiency of this material compared to pure p-Si was attributed to a higher band bending at the n^+/p interface, causing a higher difference in energy between the quasi-Fermi levels under illumination. Another approach, developed by Branz and co-workers, relied on a metal-assisted etching technique to inexpensively nanostructure the surface of a Si electrode. This was shown to greatly improve the photocathode performance by both increasing its surface area and decreasing the amount of light reflected by the surface (estimated around 25% for a planar surface).[82] Finally, Chorkendorff and co-workers reported a greatly enhanced stability toward oxidation, obtained by coating the surface of the n^+p-Si electrode with a thin layer of titanium. They also reported that MoS_x could be used as an efficient electrocatalyst with this system.[83] Overall, silicon performances as a photocathode have been recently improved using different approaches, morphology control and surface treatments, and to date, it remains one of the most promising materials for a large-scale production due to its very high abundance. Accordingly, researchers have also begun to develop oxide photoanode/p-Si photocathode tandem cells for overall water splitting. For example, very recently, a n-WO_3/p-Si device has recently been reported by Lewis and co-workers, where the semiconductors were coated on the opposite sides of the same ITO substrate.[84] While the photocurrents were low and no conversion efficiency was reported, this work critically stresses the significance of semiconductor interfaces, as these were found to limit the performance.

A last class of materials that have been studied as potential photocathodes for water reduction is the p-type metal oxides. Although studied very early, it is only recently that they achieved remarkable conversion efficiencies. Indeed, in their

dx.doi.org/10.1021/jp405291g | J. Phys. Chem. C 2013, 117, 17879–17893

early work on a variety of p-type oxides, Hardee and Bard showed that only p-CuO and p-Bi_2O_3 produced a cathodic photocurrent but were also both unstable.[85] Benko and co-workers later confirmed that, although having a low band gap (E_g = 1.35 eV) suitable for water reduction, p-CuO decomposed under illumination.[86] The first stable p-type oxide photocathode was reported by Somorjai and co-workers in 1982. In their work, they used a polycrystalline p-Fe_2O_3 electrode to reduce water, while the oxidation was performed at a polycrystalline n-Fe_2O_3 electrode. Unfortunately, the performance of the device was quite poor: only 0.06% overall conversion efficiency in 0.1 M Na_2SO_4.[87] Another stable material, crystalline p-$CaFe_2O_4$ (E_g = 1.9 eV), was later reported by Sato and co-workers but again with relatively poor performances: only a few $\mu A \cdot cm^{-2}$ under 400 mW cm^{-2} illumination.[88] Much more recently, Ishihara and co-workers reported higher photocurrents (200 μA cm^{-2}) for the same material used in tandem with an n-TiO_2 photoanode.[89] In 2008, Grimes' group reported a p−Cu−Ti−O nanotube array coupled with an n-TiO_2 photoanode.[90] The conversion efficiency of the device was reported to be 0.30%. Given the very few number of stable p-type oxides, one recent strategy has been to afford stability with surface treatments. McFarland and co-workers published the first report of a protected oxide photocathode in 2003. They used n-TiO_2 to protect an electrodeposited p-type Cu_2O (E_g = 2.0 eV) electrode.[91] By using a thin protective layer of n-TiO_2, McFarland's team showed reduced photocorrosion of the electrode without diminution of its performance. The potential of cuprous oxide as a material composed of readily available elements and the ability to be deposited at low temperature by scalable techniques (e.g., electrodeposition) has stimulated the further development of a stabilized Cu_2O electrode. Recently, Paracchino et al. reported a highly efficient electrodeposited p-Cu_2O electrode, protected by the atomic layer deposition (ALD) of nanolayers of Al-doped ZnO and TiO_2, and coated with electrodeposited platinum.[92,93] The electrode produced photocurrents as high as 7.6 $mA \cdot cm^{-2}$ at 0 V vs RHE, under standard illumination, in 1 M Na_2SO_4 (see Figure 6), and its stability has been greatly improved, from lasting only seconds without protecting layers to producing photocurrent for days with optimized protection layers. This drastic improvement in stability and the high photocurrent it has been shown to deliver makes Cu_2O arguably the state-of-the-art p-type oxide, and one of the most promising low-cost materials reported so far. Additionally, some efforts have been focused on the creation of protected p-Cu_2O electrodes evolving hydrogen without the need of expensive cocatalysts. Reisner and co-workers presented a NiO_x-coated Cu_2O photocathode, working in tandem with an n-WO_3 photoanode at pH 6,[94] and Wang and co-worker reported a carbon-protected p-Cu_2O photocathode with 0.56% conversion efficiency in 1 M Na_2SO_4 under AM 1.5 illumination.[95] Despite its recent success in the literature, it should be pointed out that, when using Cu_2O as the bottom cell in a tandem configuration, the solar-to-hydrogen conversion efficiency is limited to under 9% according to Figure 2. To achieve this performance, the top cell must have a band gap energy of exactly 2.42 eV. If used as a top cell, rather, the situation becomes less restrictive to achieve efficiency over 10%, but the availability of photoanodes with suitable band gap energy between 1.3 and 1.5 eV remains a limitation. Overall, oxide photocathodes, although considered for a long time as unstable and inefficient materials for water reduction, have recently become increasingly popular with the development of nanostructuring and protection techniques. Indeed, low-cost, solution-processed oxides represent a very attractive type of material for a large-scale device production; however, oxides with high stability and low band gap energy are generally still needed.

5. PHOTOANODE/PHOTOVOLTAIC TANDEM CELLS

Due to the difficulty in identifying stable p-type cathodes that can operate in tandem with an oxide photoelectrode to give a high performance PEC device, oxide-photoanode/photovoltaic cell tandem devices have been developed. This approach provides a good compromise between device performance, complexity, and stability. A photoelectrode/PV tandem device can be connected by simply wiring together the photoanode and PV cell, or prepared in a monolithic geometry, as shown in Figure 7. The operation conditions of a photoanode/PV

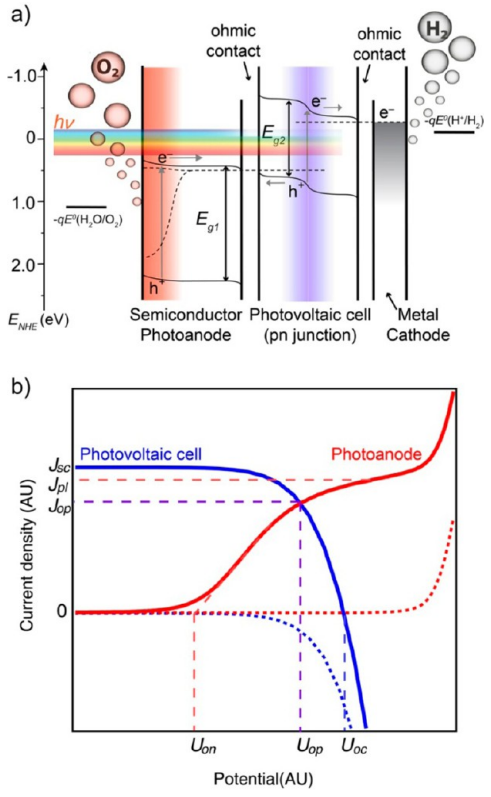

Figure 7. (a) Electron energy scheme of photoelectrode/photovoltaic tandem cells with an n-type photoanode coupled to a pn-junction photovoltaic cell. (b) The operation conditions of a photoanode/PV tandem device as shown by the idealized current−voltage curves for a PV cell (blue) on top of an n-type photoanode (red) in the dark (broken lines) and under illumination (solid lines). Relevant parameters of the curves are indicated and described in the text. Reprinted with permission from ref 111. Copyright 2010 Materials Research Society.

tandem device can be predicted by comparing the (two-electrode) current density−voltage characteristics of each individual cell under the actual illumination conditions of each separate part (given its position in the particular tandem configuration).[7] Figure 7b shows the current density, J, with respect to the applied potential (U) for an arbitrary photovoltaic cell (solid blue curve) and a photoanode (solid red curve) under illumination conditions. The operating

dx.doi.org/10.1021/jp405291g | J. Phys. Chem. C 2013, 117, 17879−17893

potential U_{op} of the tandem cell is defined as the potential measured at the intersection between the PV and the PEC cell curves. The current density (A m^{-2}) at this point, J_{op}, represents the electrical current that flows between the two cells and can be used to estimate the overall solar-to-hydrogen conversion efficiency through the following relation:

$$\eta_{STH} = \frac{J_{op}\Delta G^0_{H_2}\eta_{farad}}{2qE_S}$$

where $\Delta G^0_{H_2}$ represents the standard free energy of the hydrogen produced (lower heating value, 2.46 eV per molecule of H_2), η_{farad} is the Faradaic efficiency for the water splitting reactions, q is the elementary charge (1.6022×10^{-19} C = 1 eV V^{-1}), and E_S represents the power flux from the sun incident on the tandem cell (1000 W m^{-2} under standard conditions, AM 1.5G). The factor of 2 in the denominator represents the stoichiometric relation between one molecule of H_2 and the number of electrons needed to produce it electrochemically from H_2O. In practice, the $J-U$ properties of the individual cells can be independently varied to maximize J_{op} and, accordingly, the η_{STH} of the device.

It should be noted that, in a real device, J_{op} is not found by merely maximizing the current output from each cell (denoted as the short circuit current density, J_{sc}, for the PV cell and the plateau photocurrent density, J_{pl}, for the photoanode). U_{loss} and other device nonidealities (such as high series and low shunt resistances) necessitate that the characteristic cell potentials (denoted as the open circuit photopotential, U_{oc}, and the photocurrent onset potential, U_{on}, for the PV and the photoanode, respectively) also be considered in device optimization. Indeed, these latter parameters become the critical factors in the operation of a tandem cell. In addition, we note that the careful measurement of the photocurrent densities under standard conditions is very important for the accurate prediction of the η_{STH}. Standard methods for the measurement of PEC cells have recently been reported.[96]

To date, there have been many demonstrations of this type of device in the literature. For example, a TiO_2 photoanode in tandem with a thin film PV device based on $Cu(In,Ga)Se_2$/CdS produced hydrogen at a rate of 0.052 μL s^{-1} cm^{-2} during unassisted solar water splitting (corresponding to an IPCE of 1.02%).[97] While less interest has been paid toward using the prototypical TiO_2 as a photoanode due to its large band gap, this work demonstrated the importance of using optimized protective layers ($Nb_{0.03}Ti_{0.97}O_{1.84}$ in this case) to eliminate corrosion of the PV cell in the aqueous conditions.

Research efforts have recently focused on using promising transition metal oxides like WO_3 and Fe_2O_3. Miller and co-workers have investigated combining tungsten[98] or iron[99] oxide photoanodes in tandem with a-Si:Ge PV. As a drawback, the large overpotential for water oxidation (η_{ox}) and the relatively low U_{oc} of an a-Si device requires a double junction PV in tandem to provide sufficient potential to drive the overall water splitting reaction (similar to the PV only case where 3 pn-junctions were needed with a-Si). Despite this, 3% η_{STH} was obtained with the WO_3/a-Si:Ge/a-Si:Ge device.[98] A similar device for iron oxide with only one PV (Fe_2O_3/a-Si:Ge) did not split water without an external bias, but it was shown that a 0.65 V bias "savings" was earned under AM 1.5G illumination.[99] Likewise, a 0.3 V reduction in the necessary overpotential was noted when Fe_2O_3 was deposited on n-Si.[100]

From a practical perspective, the attractive aspects of using a widely available, highly stable, and inexpensively produced photoanode are diminished when using a tandem component that requires relatively expensive processing techniques (e.g., the plasma-enhanced chemical vapor deposition of a-Si). Thus, many investigations have focused on using next-generation photovoltaics that can also be fabricated with inexpensive, solution processing methods. The dye-sensitized solar cell (DSSC) is the prototype example[101] of this class of photovoltaic device and thus has attracted significant attention for use in solar water splitting tandem cells with a stable photoanode.[102] One important advantage of using a DSSC over that of a conventional pn-junction photovoltaic device is that the voltage output of the DSSCs is less sensitive with varying illumination intensity.[103] This implies that a photoanode/DSSC tandem cell designed to operate at 1 sun illumination will maintain sufficient $\Delta\mu_{ex}$ for water splitting compared to a photoanode/pn-junction combination during conditions of lower light intensities (e.g., during hazy or partially cloudy days).

The photoanode/DSSC combination was first suggested by Augustynski and Grätzel[104] with WO_3 as the photoanode—suggesting that device would be capable of 4.5% η_{STH} based on the plateau photocurrent (J_{pl}) of WO_3.[105] In practice, tandem devices with WO_3 have been constructed by Park and Bard[106] and Arakawa et al.[107] giving η_{STH}'s up to 2.8% at AM 1.5G (100 mW cm^{-2}) using Pt as the cathode. However, similar to the a-Si based devices, two DSSCs connected in series to the photoanode were necessary to afford overall water splitting. This was accomplished by positioning these two DSSCs side by side behind the WO_3 photoanode.

This photoanode/2×DSSC architecture does not fundamentally provide a limitation to the possible solar-to-hydrogen conversion efficiency compared to a two-absorber D4 approach for WO_3 or even the more promising Fe_2O_3, as less than one-third of the available solar photons have a wavelength shorter than 600 nm and pan-chromatic dyes with high quantum efficiency extending past 900 nm are being developed.[108] However, it does present a challenge to device construction as the two DSCs need to be constructed each with half of the active area of the photoanode in order to normalize the total area of the device.

The development of new dyes for the DSSC during the past decade has initiated work to explore alternative device architectures for optimizing light harvesting in these water splitting tandem cells. For example, all-organic dyes, such as the squaraine dye, have a narrow absorption bandwidth extending into the far red region of the visible, and have demonstrated solar power conversion efficiencies over 6% under AM 1.5G illumination.[109,110] Specifically, the dye coded SQ1 absorbs light with wavelengths only between 550 and 700 nm. In addition to considerably reducing costs when compared to a ruthenium-based dye, Brillet et al. pointed out that two new distinct tandem cell configurations become accessible when using this type of dye.[111] The possible configurations are shown in Figure 8. In addition to the standard photoanode/2×DSSC design (Figure 8a), a true trilevel device (photoanode/squaraine DSSC/panchromatic DSSC) would also be effective (Figure 8b). This configuration would eliminate the need to construct two DSSCs side by side. A second additional possibility is to arrange two side-by-side DSSCs in front of a hematite photoanode (Figure 8c). This "front DSSC" configuration is particularly attractive in view of light harvesting

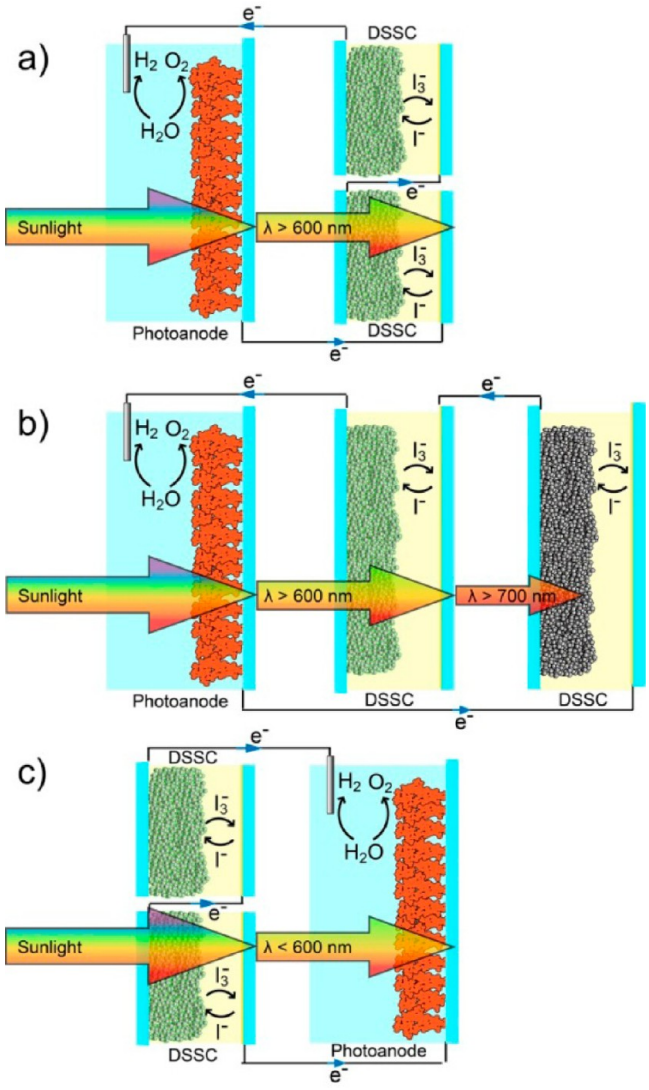

Figure 8. Layout of three architectures for a tandem cell using a hematite photoanode and two dye-sensitized solar cells in series. (a) "back DSSC" configuration, (b) "trilevel" configuration, and (c) "front DSSC" configuration. Reprinted with permission from ref 111. Copyright 2010 Materials Research Society.

as transition metal oxides (in particular hematite) have high indexes of refraction, which increase reflection. Moreover, the front DSSC approach eliminates the need to deposit the photoanode on a transparent conducting glass and an inexpensive metal foil support could instead be used.

Brillet et al. determined how these two new photoanode/DSSC tandem concepts performed compared to the standard architecture using nanostructured hematite photoanodes. The trilevel tandem architecture (photoanode/squaraine DSSC/panchromatic DSSC) produced the highest operating current density, and thus the highest expected solar-to-hydrogen efficiency of 1.36%. The conventional photoanode/2×DSSC architecture gave 1.16%, and the front DSSC configuration resulted in 0.76%. It should be noted that these values were far below the expected 3.3% that should have been possible with the nanostructured hematite photoanodes used. Reduced light harvesting caused by scattering and reflection were strongly affecting the overall conversion efficiency. This is illustrated by the optical and electronic characteristics of the trilevel tandem cell presented in Figure 9. Here, it is shown that, while the hematite photoanode only produces photocurrent for λ < 600 nm, the light transmitted to the middle and back cells is severely attenuated by scattering and reflection losses. This causes the DSSC photocurrent to limit the overall performance of the tandem cell. While device engineering should improve the operating current density by reducing reflection, scattering, and resistive losses, DSSCs with higher U_{oc}'s would enable a true D4 photoanode/DSSC water splitting tandem cell.

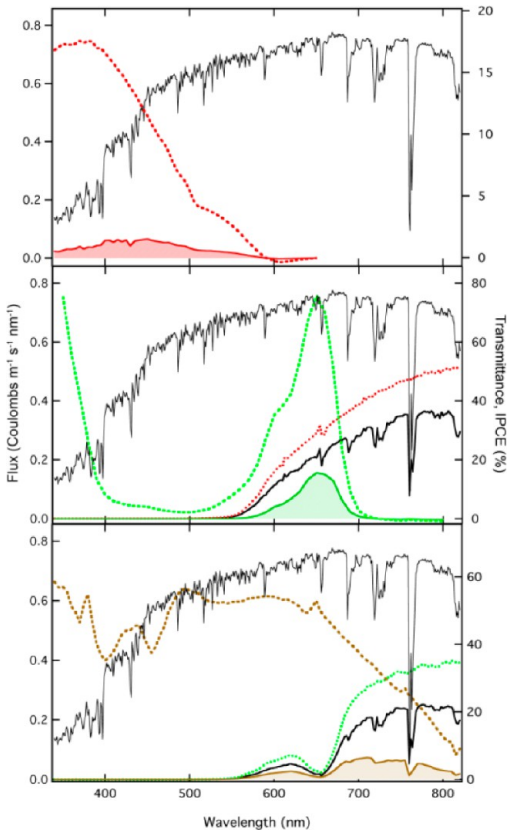

Figure 9. Optical and electronic characteristics of the "trilevel" tandem cell. Top panel: The solid line shows the incident solar flux. The IPCE of the hematite (dashed line) is convoluted with the solar flux to give the electron flux in the photoanode (shaded area). Middle panel: The solar flux is convoluted with the transmittance of the hematite (dotted line) to give the incident irradiance on the squaraine DSSC (solid bold line). The irradiance is convoluted with the IPCE of the squaraine DSSC (dashed line) to give the electron flux in the intermediate photovoltaic device (shaded area). Bottom panel: The solar flux is convoluted with the transmittance of the squaraine dye plus hematite (dotted line) to give the incident irradiance on the black DSSC (solid bold line). The irradiance is convoluted with the IPCE of the black DSSC (dashed line) to give the electron flux in the bottom photovoltaic device (shaded area). Reprinted with permission from ref 111. Copyright 2010 Materials Research Society.

Indeed, in 2012, a specifically designed cobalt redox couple combined with an all-organic dye (coded Y123) gave DSSCs with U_{oc} > 1.0 V at 1 sun conditions.[112] This breakthrough allowed the first demonstration of a D4 photoanode/DSSC water splitting tandem cell.[113] Devices were assembled with both nanostructured WO_3 and Fe_2O_3 photoandes, and J_{op} was measured to give η_{STH} values of 3.10 and 1.17% with the WO_3/DSSC and Fe_2O_3/DSSC combinations, respectively. An optical analysis also compared the predicted photocurrent from the

dx.doi.org/10.1021/jp405291g | J. Phys. Chem. C 2013, 117, 17879−17893

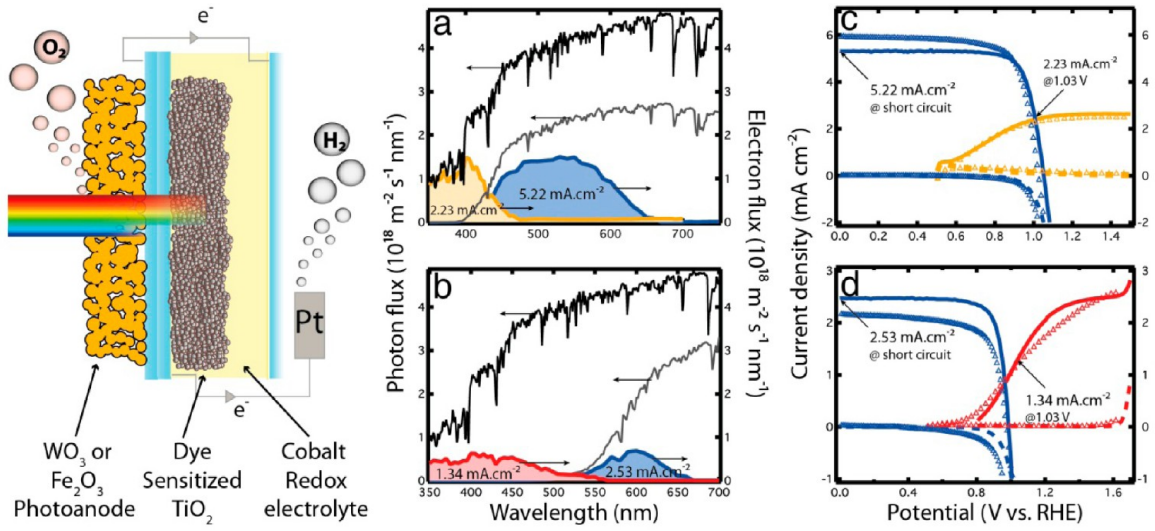

Figure 10. General scheme (left) of a photoanode/dye-sensitized-solar-cell tandem cell. Spectral response and $J-V$ characteristics of the WO_3 (yellow)/DSSC (blue) (a, c) and Fe_2O_3 (red)/DSSC (blue) (b, d) tandem cells. The transmittance of the photoanode (not shown) convoluted to the AM 1.5G photon flux on the photoanode (a, b black lines) allows the calculation of the photon flux incident to the DSSC (a, b gray lines). IPCE data (not shown) and the photon flux incident to each element are used to estimate the photocurrent density (shaded areas under the curves in parts a and b). $J-V$ curves (c and d) of the cells are shown under AM 1.5G irradiation. The filled lines represent the $J-V$ curves predicted from calculation (see ref), and the triangles represent data from in situ device measurements. Adapted from ref 113.

integration of IPCE measurements and the actual $J-U$ behavior measured *in situ* in the device. This optical analysis and the $J-U$ curves for each device are shown in Figure 10. In the case of the Fe_2O_3/DSSC tandem cell, J_{op} is far from the plateau region of the hematite electrode photocurrent. This results in a performance far from the maximum obtainable. The limitation of this system is clearly the late onset of the photocurrent in the photoelectrode, despite the use of state-of-the-art strategies to shift cathodically the onset of the photocurrent by means of surface catalysis and passivation. However, in the case of the WO_3/DSSC tandem cell, the photocurrent onset is not a limitation and the J_{op} is very close to the plateau region of the photoanode (approximately 1000 mV). The limiting factor in this case is the low photocurrent obtainable by the photoanode due to the less than ideal absorption capability of tungsten trioxide in the visible region of the solar spectrum. Despite this, the Fe_2O_3/DSSC device still exhibited a near unity faradaic efficiency and a good stability over an 8 h testing period. Overall, this work suggests that the low η_{STH} of the D4 hematite/DSSC tandem cell offers the larger room for improvement, in particular, further reduction of the overpotential for water oxidation.

6. CONCLUSIONS AND OUTLOOK

Since the discovery of water photoelectrolysis as an attractive way to produce solar hydrogen, numerous cell designs have been suggested and investigated. Due to limitations in identifying ideal materials, the original single-absorber (S2) approach to achieve direct solar energy conversion has given way to the more efficient dual-absorber (D4) configuration. Using two absorbing materials indeed allows for better light harvesting properties, and better stability as the two sides of the cell are subject to different conditions and can be optimized separately. It has been further shown that placing two photoelectrodes one on top of the other allowed for higher theoretical maximum efficiencies than a "side-by-side" design (21.6 vs 16.6%), notably thanks to a reduction by half of the surface area of the device.

The practical realization of a wireless integrated tandem device composed of two semiconductor photoelectrodes comes with different issues to overcome, among which are the stability of the photoelectrodes, the poor kinetics of the water splitting half-reactions, and the cost of production. However, recent advances in protection and nanostructuring techniques have allowed the creation of increasingly efficient and robust photoelectrodes based on earth-abundant materials, through a better control of the size and shape of the materials on a microscopic level. However, long-term stability and the further reduction of electrochemical overpotentials remain major challenges in the development of photoelectrodes. The development of photocathode materials is comparably immature to that of their photoanode counterparts, and the identification of intrinsically stable photocathode material with a band gap energy in the 1.2−1.4 eV range is urgently needed.

An alternative tandem-cell design is to combine a photoelectrode with a photovoltaic device. This approach was initially not favored, due to the need to have several photovoltaic junctions to achieve a high enough voltage to split water, the often poor stability of the materials in aqueous conditions, and their relatively high cost. However, recent progress with high-voltage dye-sensitized solar cells has allowed the demonstration of a cheap photo-electrocatalytic cell, composed of one oxide photoanode and one DSSC connected together.

After 40 years of research, and thanks to great advances in the fields of nanotechnology, materials science, and electrochemistry, the goal of an efficient and stable tandem cell based on cheap and abundant materials seems to be within reach. While long-term stability and higher solar-to-hydrogen conversion efficiency are still needed, the recent and rapid development of new photoelectrode materials like $BiVO_4$, and robust, strongly absorbing organic dyes for the DSSC,[114] along with the continued understanding of the photoelectrochemical processes occurring at the electrodes,[60] suggest that these

dx.doi.org/10.1021/jp405291g | J. Phys. Chem. C 2013, 117, 17879−17893

remaining challenges can be overcome. The next decades will likely bring PEC development to economically viable solar fuel production by water splitting and the commercialization of this technology on which global-scale solar energy storage and "solar refineries" can be based.

AUTHOR INFORMATION

Corresponding Author

*E-mail: kevin.sivula@epfl.ch. Phone: +41 21 693 79 79.

Notes

The authors declare no competing financial interest.

Biographies

Mathieu S. Prévot obtained his MSc in matter sciences from the Ecole Normale Supérieure de Lyon in 2012 after two research internships at the University of Calgary. He was accepted as a PhD student in the Laboratory for Molecular Engineering of Optoelectronic Nanomaterials at EPFL in 2013.

Kevin Sivula obtained a PhD in chemical engineering from UC Berkeley in 2007. In 2012, after leading a research group in the Laboratory of Photonics and Interfaces at EPFL, he was appointed tenure track assistant professor. He now heads the Laboratory for Molecular Engineering of Optoelectronic Nanomaterials (http://limno.epfl.ch) at EPFL.

ACKNOWLEDGMENTS

The Faculty of Basic Sciences at EPFL and the EOS holdings (contract number 536067) are acknowledged for providing financial support.

REFERENCES

(1) Schlögl, R. The Role of Chemistry in the Energy Challenge. *ChemSusChem* **2010**, *3*, 209−222.

(2) Olateju, B.; Kumar, A. Techno-Economic Assessment of Hydrogen Production from Underground Coal Gasification (UCG) in Western Canada with Carbon Capture and Sequestration (CCS) for Upgrading Bitumen from Oil Sands. *Appl. Energy* **2013**, *111*, 428−440.

(3) Dutta, S. Technology Assessment of Advanced Electrolytic Hydrogen Production. *Int. J. Hydrogen Energy* **1990**, *15*, 379−386.

(4) Committee on Alternatives and Strategies for Future Hydrogen Production and Use, N. R. C., National Academy of Engineering. *The Hydrogen Economy: Opportunities, Costs, Barriers, and R&D Needs*; National Academies Press: Washington, DC, 2004.

(5) Goodrich, A.; James, T.; Woodhouse, M. Residential, Commercial, and Utility-Scale Photovoltaic (PV) System Prices in the United States: Current Drivers and Cost Reduction Opportunities; NREL/TP-6A20-53347L; National Renewable Energy Laboratory: Golden, CO, 2012.

(6) Fujishima, A.; Honda, K. Electrochemical Photolysis of Water at a Semiconductor Electrode. *Nature* **1972**, *238*, 37−39.

(7) Weber, M. F.; Dignam, M. J. Efficiency of Splitting Water with Semiconducting Photoelectrodes. *J. Electrochem. Soc.* **1984**, *131*, 1258−1265.

(8) Bolton, J. R.; Strickler, S. J.; Connolly, J. S. Limiting and Realizable Efficiencies of Solar Photolysis of Water. *Nature* **1985**, *316*, 495−500.

(9) Bolton, J. R. Solar Photoproduction of Hydrogen: A Review. *Solar Energy* **1996**, *57*, 37−50.

(10) ASTM Standard G173 - 03, 2008, "Standard Tables for Reference Solar Spectral Irradiances: Direct Normal and Hemispherical on 37° Tilted Surface", ASTM International, West Conshohocken, PA, 2008, DOI: 10.1520/G0173-03R08, www.astm.org.

(11) Hu, S.; Xiang, C.; Haussener, S.; Berger, A. D.; Lewis, N. S. An Analysis of the Optimal Band Gaps of Light Absorbers in Integrated Tandem Photoelectrochemical Water-Splitting Systems. *Energy Environ. Sci.* **2013**, DOI: 10.1039/c3ee40453f.

(12) Kelly, N.; Gibson, T.; Ouwerkerk, D. A Solar-Powered, High-Efficiency Hydrogen Fueling System Using High-Pressure Electrolysis of Water: Design and Initial Results. *Int. J. Hydrogen Energy* **2008**, *33*, 2747−2764.

(13) Khaselev, O.; Turner, J. A. A Monolithic Photovoltaic-Photoelectrochemical Device for Hydrogen Production via Water Splitting. *Science* **1998**, *280*, 425−427.

(14) Khaselev, O.; Turner, J. A. Electrochemical Stability of p-$GaInP_2$ in Aqueous Electrolytes toward Photoelectrochemical Water Splitting. *J. Electrochem. Soc.* **1998**, *145*, 3335−3339.

(15) Fujishima, A.; Zhang, X. T.; Tryk, D. A. TiO_2 Photocatalysis and Related Surface Phenomena. *Surf. Sci. Rep.* **2008**, *63*, 515−582.

(16) Ghosh, A. K.; Maruska, H. P. Photoelectrolysis of Water in Sunlight with Sensitized Semiconductor Electrodes. *J. Electrochem. Soc.* **1977**, *124*, 1516−1522.

(17) Nowotny, J.; Bak, T.; Nowotny, M. K.; Sheppard, L. R. Titanium Dioxide for Solar-Hydrogen I. Functional Properties. *Int. J. Hydrogen Energy* **2007**, *32*, 2609−2629.

(18) Chen, X.; Liu, L.; Yu, P. Y.; Mao, S. S. Increasing Solar Absorption for Photocatalysis with Black Hydrogenated Titanium Dioxide Nanocrystals. *Science* **2011**, *331*, 746−750.

(19) Zhang, Q.; Lima, D. Q.; Lee, I.; Zaera, F.; Chi, M.; Yin, Y. A Highly Active Titanium Dioxide Based Visible-Light Photocatalyst with Nonmetal Doping and Plasmonic Metal Decoration. *Angew. Chem., Int. Ed.* **2011**, *50*, 7088−7092.

(20) Linic, S.; Christopher, P.; Ingram, D. B. Plasmonic-Metal Nanostructures for Efficient Conversion of Solar to Chemical Energy. *Nat. Mater.* **2011**, *10*, 911−921.

(21) Liu, Z.; Hou, W.; Pavaskar, P.; Aykol, M.; Cronin, S. B. Plasmon Resonant Enhancement of Photocatalytic Water Splitting Under Visible Illumination. *Nano Lett.* **2011**, *11*, 1111−1116.

(22) Zhou, X.; Liu, G.; Yu, J.; Fan, W. Surface Plasmon Resonance-Mediated Photocatalysis by Noble Metal-Based Composites under Visible Light. *J. Mater. Chem.* **2012**, *22*, 21337−21354.

(23) Sartoretti, C. J.; Alexander, B. D.; Solarska, R.; Rutkowska, W. A.; Augustynski, J.; Cerny, R. Photoelectrochemical Oxidation of Water at Transparent Ferric Oxide Film Electrodes. *J. Phys. Chem. B* **2005**, *109*, 13685−13692.
(24) Sayama, K.; Nomura, A.; Zou, Z.; Abe, R.; Abe, Y.; Arakawa, H. Photoelectrochemical Decomposition of Water on Nanocrystalline $BiVO_4$ Film Electrodes under Visible Light. *Chem. Commun. (Cambridge, U. K.)* **2003**, *0*, 2908−2909.
(25) Sivula, K.; Le Formal, F.; Grätzel, M. Solar Water Splitting: Progress Using Hematite (α-Fe_2O_3) Photoelectrodes. *ChemSusChem* **2011**, *4*, 432−449.
(26) Mi, Q.; Zhanaidarova, A.; Brunschwig, B. S.; Gray, H. B.; Lewis, N. S. A Quantitative Assessment of the Competition between Water and Anion Oxidation at WO_3 Photoanodes in Acidic Aqueous Electrolytes. *Energy Environ. Sci.* **2012**, *5*, 5694−5700.
(27) Butler, M. A. Photoelectrolysis and Physical-Properties of Semiconducting Electrode WO_3. *J. Appl. Phys.* **1977**, *48*, 1914−1920.
(28) Solarska, R.; Alexander, B. D.; Braun, A.; Jurczakowski, R.; Fortunato, G.; Stiefel, M.; Graule, T.; Augustynski, J. Tailoring the Morphology of WO_3 Films with Substitutional Cation Doping: Effect on the Photoelectrochemical Properties. *Electrochim. Acta* **2010**, *55*, 7780−7787.
(29) Solarska, R.; Królikowska, A.; Augustyński, J. Silver Nanoparticle Induced Photocurrent Enhancement at WO_3 Photoanodes. *Angew. Chem., Int. Ed.* **2010**, *49*, 7980−7983.
(30) Janáky, C.; Rajeshwar, K.; de Tacconi, N. R.; Chanmanee, W.; Huda, M. N. Tungsten-Based Oxide Semiconductors for Solar Hydrogen Generation. *Catal. Today* **2013**, *199*, 53−64.
(31) Kudo, A.; Omori, K.; Kato, H. A Novel Aqueous Process for Preparation of Crystal Form-Controlled and Highly Crystalline $BiVO_4$ Powder from Layered Vanadates at Room Temperature and Its Photocatalytic and Photophysical Properties. *J. Am. Chem. Soc.* **1999**, *121*, 11459−11467.
(32) Ye, H.; Lee, J.; Jang, J. S.; Bard, A. J. Rapid Screening of $BiVO_4$-Based Photocatalysts by Scanning Electrochemical Microscopy (SECM) and Studies of Their Photoelectrochemical Properties. *J. Phys. Chem. C* **2010**, *114*, 13322−13328.
(33) Li, M.; Zhao, L.; Guo, L. Preparation and Photoelectrochemical Study of $BiVO_4$ Thin Films Deposited by Ultrasonic Spray Pyrolysis. *Int. J. Hydrogen Energy* **2010**, *35*, 7127−7133.
(34) Yao, W.; Iwai, H.; Ye, J. Effects of Molybdenum Substitution on the Photocatalytic Behavior of $BiVO_4$. *Dalton Trans.* **2008**, 1426−1430.
(35) Luo, W.; Yang, Z.; Li, Z.; Zhang, J.; Liu, J.; Zhao, Z.; Wang, Z.; Yan, S.; Yu, T.; Zou, Z. Solar Hydrogen Generation from Seawater with a Modified $BiVO_4$ Photoanode. *Energy Environ. Sci.* **2011**, *4*, 4046−4051.
(36) Pilli, S. K.; Furtak, T. E.; Brown, L. D.; Deutsch, T. G.; Turner, J. A.; Herring, A. M. Cobalt-Phosphate (Co-Pi) Catalyst Modified Mo-Doped $BiVO_4$ Photoelectrodes for Solar Water Oxidation. *Energy Environ. Sci.* **2011**, *4*, 5028−5034.
(37) Zhong, D. K.; Choi, S.; Gamelin, D. R. Near-Complete Suppression of Surface Recombination in Solar Photoelectrolysis by "Co-Pi" Catalyst-Modified W:$BiVO_4$. *J. Am. Chem. Soc.* **2011**, *133*, 18370−18377.
(38) Abdi, F. F.; van de Krol, R. Nature and Light Dependence of Bulk Recombination in Co-Pi-Catalyzed $BiVO_4$ Photoanodes. *J. Phys. Chem. C* **2012**, *116*, 9398−9404.
(39) Dotan, H.; Sivula, K.; Gratzel, M.; Rothschild, A.; Warren, S. C. Probing the Photoelectrochemical Properties of Hematite (α-Fe_2O_3) Electrodes Using Hydrogen Peroxide as a Hole Scavenger. *Energy Environ. Sci.* **2011**, *4*, 958−964.
(40) Hardee, K. L.; Bard, A. J. Semiconductor Electrodes 5. Application of Chemically Vapor-Deposited Iron-Oxide Films to Photosensitized Electrolysis. *J. Electrochem. Soc.* **1976**, *123*, 1024−1026.
(41) Kennedy, J. H.; Frese, K. W. Photo-Oxidation of Water at alpha-Fe_2O_3 Electrodes. *J. Electrochem. Soc.* **1978**, *125*, 709−714.
(42) Dareedwards, M. P.; Goodenough, J. B.; Hamnett, A.; Trevellick, P. R. Electrochemistry and Photoelectrochemistry of Iron(III) Oxide. *J. Chem. Soc., Faraday Trans.* **1983**, *79*, 2027−2041.
(43) Sanchez, C.; Sieber, K. D.; Somorjai, G. A. The Photoelectrochemistry of Niobium Doped Alpha-Fe_20_3. *J. Electroanal. Chem.* **1988**, *252*, 269−290.
(44) Itoh, K.; Bockris, J. O. Stacked Thin-Film Photoelectrode Using Iron-Oxide. *J. Appl. Phys.* **1984**, *56*, 874−876.
(45) Itoh, K.; Bockris, J. O. Thin-Film Photoelectrochemistry - Iron-Oxide. *J. Electrochem. Soc.* **1984**, *131*, 1266−1271.
(46) Horowitz, G. Capacitance Voltage Measurements and Flat-Band Potential Determination on Zr-Doped Alpha-Fe_2O_3 Single-Crystal Electrodes. *J. Electroanal. Chem.* **1983**, *159*, 421−436.
(47) Tilley, S.; Cornuz, M.; Sivula, K.; Grätzel, M. Light-Induced Water Splitting with Hematite: Improved Nanostructure and Iridium Oxide Catalysis. *Angew. Chem., Int. Ed.* **2010**, *49*, 6405−6408.
(48) Brillet, J.; Grätzel, M.; Sivula, K. Decoupling Feature Size and Functionality in Solution-Processed, Porous Hematite Electrodes for Solar Water Splitting. *Nano Lett.* **2010**, *10*, 4155−4160.
(49) Gonçalves, R. H.; Lima, B. H. R.; Leite, E. R. Magnetite Colloidal Nanocrystals: A Facile Pathway to Prepare Mesoporous Hematite Thin Films for Photoelectrochemical Water Splitting. *J. Am. Chem. Soc.* **2011**, *133*, 6012−6019.
(50) Sivula, K.; Le Formal, F.; Gratzel, M. WO_3-Fe_2O_3 Photoanodes for Water Splitting: A Host Scaffold, Guest Absorber Approach. *Chem. Mater.* **2009**, *21*, 2862−2867.
(51) Lin, Y.; Zhou, S.; Sheehan, S. W.; Wang, D. Nanonet-Based Hematite Heteronanostructures for Efficient Solar Water Splitting. *J. Am. Chem. Soc.* **2011**, *133*, 2398−2401.
(52) Stefik, M.; Cornuz, M.; Mathews, N.; Hisatomi, T.; Mhaisalkar, S.; Grätzel, M. Transparent, Conducting Nb:SnO_2 for Host−Guest Photoelectrochemistry. *Nano Lett.* **2012**, *12*, 5431−5435.
(53) Liang, Y. Q.; Enache, C. S.; van de Krol, R. Photoelectrochemical Characterization of Sprayed Alpha-Fe2O3 Thin Films: Influence of Si Doping and SnO_2 Interfacial Layer. *Int. J. Photoenergy* **2008**, 739864.
(54) Hisatomi, T.; Dotan, H.; Stefik, M.; Sivula, K.; Rothschild, A.; Grätzel, M.; Mathews, N. Enhancement in the Performance of Ultrathin Hematite Photoanode for Water Splitting by an Oxide Underlayer. *Adv. Mater.* **2012**, *24*, 2699−2702.
(55) Hisatomi, T.; Brillet, J.; Cornuz, M.; Le Formal, F.; Tetreault, N.; Sivula, K.; Gratzel, M. A Ga_2O_3 Underlayer as an Isomorphic Template for Ultrathin Hematite Films toward Efficient Photoelectrochemical Water Splitting. *Faraday Discuss.* **2012**, *155*, 223−232.
(56) Le Formal, F.; Grätzel, M.; Sivula, K. Controlling Photoactivity in Ultrathin Hematite Films for Solar Water-Splitting. *Adv. Funct. Mater.* **2010**, *20*, 1099−1107.
(57) McDonald, K. J.; Choi, K.-S. Synthesis and Photoelectrochemical Properties of Fe2O3/ZnFe2O4 Composite Photoanodes for Use in Solar Water Oxidation. *Chem. Mater.* **2011**, *23*, 4863−4869.
(58) Sivula, K.; Zboril, R.; Le Formal, F.; Robert, R.; Weidenkaff, A.; Tucek, J.; Frydrych, J.; Grätzel, M. Photoelectrochemical Water Splitting with Mesoporous Hematite Prepared by a Solution-Based Colloidal Approach. *J. Am. Chem. Soc.* **2010**, *132*, 7436−7444.
(59) Frydrych, J.; Machala, L.; Tucek, J.; Siskova, K.; Filip, J.; Pechousek, J.; Safarova, K.; Vondracek, M.; Seo, J. H.; Schneeweiss, O.; Gratzel, M.; Sivula, K.; Zboril, R. Facile Fabrication of Tin-Doped Hematite Photoelectrodes - Effect of Doping On Magnetic Properties and Performance for Light-Induced Water Splitting. *J. Mater. Chem.* **2012**, *22*, 23232−23239.
(60) Sivula, K. Metal Oxide Photoelectrodes for Solar Fuel Production, Surface Traps, and Catalysis. *J. Phys. Chem. Lett.* **2013**, *4*, 1624−1633.
(61) Klahr, B. M.; Hamann, T. W. Current and Voltage Limiting Processes in Thin Film Hematite Electrodes. *J. Phys. Chem. C* **2011**, *115*, 8393−8399.
(62) Le Formal, F.; Tetreault, N.; Cornuz, M.; Moehl, T.; Gratzel, M.; Sivula, K. Passivating Surface States on Water Splitting Hematite Photoanodes with Alumina Overlayers. *Chem. Sci.* **2011**, *2*, 737−743.

(63) Hisatomi, T.; Le Formal, F.; Cornuz, M.; Brillet, J.; Tetreault, N.; Sivula, K.; Gratzel, M. Cathodic Shift in Onset Potential of Solar Oxygen Evolution on Hematite by 13-Group Oxide Overlayers. *Energy Environ. Sci.* **2011**, *4*, 2512−2515.
(64) Le Formal, F.; Sivula, K.; Grätzel, M. The Transient Photocurrent and Photovoltage Behavior of a Hematite Photoanode under Working Conditions and the Influence of Surface Treatments. *J. Phys. Chem. C* **2012**, *116*, 26707−26720.
(65) Gamelin, D. R. Water Splitting: Catalyst or Spectator? *Nat. Chem.* **2012**, *4*, 965−967.
(66) Osterloh, F. E.; Parkinson, B. A. Recent Developments in Solar Water-Splitting Photocatalysis. *MRS Bull.* **2011**, *36*, 17−22.
(67) Yoneyama, H.; Sakamoto, H.; Tamura, H. A Photo-Electochemical Cell with Production of Hydrogen and Oxygen by a Cell Reaction. *Electrochim. Acta* **1975**, *20*, 341−345.
(68) Ohashi, K.; McCann, J.; Bockris, J. O. M. Stable Photo-electrochemical Cells for the Splitting of Water. *Nature* **1977**, *266*, 610−611.
(69) Aharon-Shalom, E.; Heller, A. Efficient p-InP(Rh-Halloy) and p-InP(Re-Halloy) Hydrogen Evolving Photocathodes. *J. Electrochem. Soc.* **1982**, *129*, 2865−2866.
(70) Kainthla, R. C.; Zelenay, B.; Bockris, J. O. M. Significant Efficiency Increase in Self-Driven Photoelectrochemical Cell for Water Photoelectrolysis. *J. Electrochem. Soc.* **1987**, *134*, 841−845.
(71) Ohashi, K.; Uosaki, K.; Bockris, J. O. M. Cathodes for Photodriven Hydrogen Generators: Znte and Cdte. *Int. J. Energy Res.* **1977**, *1*, 25−30.
(72) Baglio, J. A.; Calabrese, G. S.; Harrison, D. J.; Kamieniecki, E.; Ricco, A. J.; Wrighton, M. S.; Zoski, G. D. Electrochemical Characterization of p-Type Semiconducting Tungsten Disulfide Photocathodes: Efficient Photoreduction Processes at Semiconductor/Liquid Electrolyte Interfaces. *J. Am. Chem. Soc.* **1983**, *105*, 2246−2256.
(73) McKone, J. R.; Pieterick, A. P.; Gray, H. B.; Lewis, N. S. Hydrogen Evolution from Pt/Ru-Coated p-Type WSe2 Photocathodes. *J. Am. Chem. Soc.* **2013**, *135*, 223−231.
(74) Yokoyama, D.; Minegishi, T.; Maeda, K.; Katayama, M.; Kubota, J.; Yamada, A.; Konagai, M.; Domen, K. Photoelectrochemical Water Splitting Using a Cu(In,Ga)Se_2 Thin Film. *Electrochem. Commun.* **2010**, *12*, 851−853.
(75) Moriya, M.; Minegishi, T.; Kumagai, H.; Katayama, M.; Kubota, J.; Domen, K. Stable Hydrogen Evolution from CdS-Modified $CuGaSe_2$ Photoelectrode under Visible-Light Irradiation. *J. Am. Chem. Soc.* **2013**, *135*, 3733−3735.
(76) Marsen, B.; Cole, B.; Miller, E. L. Photoelectrolysis of Water Using Thin Copper Gallium Diselenide Electrodes. *Sol. Energy Mater. Sol. Cells* **2008**, *92*, 1054−1058.
(77) Ikeda, S.; Nonogaki, M.; Septina, W.; Gunawan, G.; Harada, T.; Matsumura, M. Fabrication of $CuInS_2$ and Cu(In,Ga)S_2 Thin Films by a Facile Spray Pyrolysis and Their Photovoltaic and Photoelectrochemical Properties. *Catal. Sci. Technol.* **2013**, *3*, 1849−1854.
(78) Candea, R. M.; Kastner, M.; Goodman, R.; Hickok, N. Photoelectrolysis of Water: Si in Salt Water. *J. Appl. Phys.* **1976**, *47*, 2724−2726.
(79) Bookbinder, D. C.; Bruce, J. A.; Dominey, R. N.; Lewis, N. S.; Wrighton, M. S. Synthesis and Characterization of a Photosensitive Interface for Hydrogen Generation: Chemically Modified P-Type Semiconducting Silicon Photocathodes. *Proc. Natl. Acad. Sci. U.S.A.* **1980**, *77*, 6280−6284.
(80) Nakato, Y.; Egi, Y.; Hiramoto, M.; Tsubomura, H. Hydrogen Evolution and Iodine Reduction on an Illuminated n-p Junction Silicon Electrode and Its Application to Efficient Solar Photoelectrolysis of Hydrogen Iodide. *J. Phys. Chem.* **1984**, *88*, 4218−4222.
(81) Boettcher, S. W.; Warren, E. L.; Putnam, M. C.; Santori, E. A.; Turner-Evans, D.; Kelzenberg, M. D.; Walter, M. G.; McKone, J. R.; Brunschwig, B. S.; Atwater, H. A.; Lewis, N. S. Photoelectrochemical Hydrogen Evolution Using Si Microwire Arrays. *J. Am. Chem. Soc.* **2011**, *133*, 1216−1219.
(82) Oh, J.; Deutsch, T. G.; Yuan, H.-C.; Branz, H. M. Nanoporous Black Silicon Photocathode for H_2 Production by Photoelectrochemical Water Splitting. *Energy Environ. Sci.* **2011**, *4*, 1690−1694.
(83) Seger, B.; Laursen, A. B.; Vesborg, P. C. K.; Pedersen, T.; Hansen, O.; Dahl, S.; Chorkendorff, I. Hydrogen Production Using a Molybdenum Sulfide Catalyst on a Titanium-Protected n+p-Silicon Photocathode. *Angew. Chem., Int. Ed.* **2012**, *51*, 9128−9131.
(84) Coridan, R. H.; Shaner, M.; Wiggenhorn, C.; Brunschwig, B. S.; Lewis, N. S. Electrical and Photoelectrochemical Properties of WO_3/Si Tandem Photoelectrodes. *J. Phys. Chem. C* **2013**, *117*, 6949−6957.
(85) Hardee, K. L.; Bard, A. J. Semiconductor Electrodes: X . Photoelectrochemical Behavior of Several Polycrystalline Metal Oxide Electrodes in Aqueous Solutions. *J. Electrochem. Soc.* **1977**, *124*, 215−224.
(86) Koffyberg, F. P.; Benko, F. A. A Photoelectrochemical Determination of the Position of the Conduction and Valence Band Edges of p-Type CuO. *J. Appl. Phys.* **1982**, *53*, 1173−1177.
(87) Leygraf, C.; Hendewerk, M.; Somorjai, G. A. Photocatalytic Production of Hydrogen from Water by a p- and n-Type Polycrystalline Iron Oxide Assembly. *J. Phys. Chem.* **1982**, *86*, 4484−4485.
(88) Matsumoto, Y.; Sugiyama, K.; Sato, E. Photocathodic Hydrogen Evolution Reactions at p-Type $CaFe_2O_4$ Electrodes with Fermi Level Pinning. *J. Electrochem. Soc.* **1988**, *135*, 98−104.
(89) Ida, S.; Yamada, K.; Matsunaga, T.; Hagiwara, H.; Matsumoto, Y.; Ishihara, T. Preparation of p-Type $CaFe_2O_4$ Photocathodes for Producing Hydrogen from Water. *J. Am. Chem. Soc.* **2010**, *132*, 17343−17345.
(90) Mor, G. K.; Varghese, O. K.; Wilke, R. H. T.; Sharma, S.; Shankar, K.; Latempa, T. J.; Choi, K.-S.; Grimes, C. A. p-Type Cu−Ti−O Nanotube Arrays and Their Use in Self-Biased Heterojunction Photoelectrochemical Diodes for Hydrogen Generation. *Nano Lett.* **2008**, *8*, 1906−1911.
(91) Siripala, W.; Ivanovskaya, A.; Jaramillo, T. F.; Baeck, S.-H.; McFarland, E. W. A Cu2O/TiO2 Heterojunction Thin Film Cathode for Photoelectrocatalysis. *Sol. Energy Mater. Sol. Cells* **2003**, *77*, 229−237.
(92) Paracchino, A.; Laporte, V.; Sivula, K.; Grätzel, M.; Thimsen, E. Highly Active Oxide Photocathode for Photoelectrochemical Water Reduction. *Nat. Mater.* **2011**, *10*, 456−461.
(93) Paracchino, A.; Mathews, N.; Hisatomi, T.; Stefik, M.; Tilley, S. D.; Gratzel, M. Ultrathin Films on Copper(I) Oxide Water Splitting Photocathodes: A Study on Performance and Stability. *Energy Environ. Sci.* **2012**, *5*, 8673−8681.
(94) Lin, C.-Y.; Lai, Y.-H.; Mersch, D.; Reisner, E. Cu_2O|NiO_x Nanocomposite as an Inexpensive Photocathode In Photoelectrochemical Water Splitting. *Chem. Sci.* **2012**, *3*, 3482−3487.
(95) Zhang, Z.; Dua, R.; Zhang, L.; Zhu, H.; Zhang, H.; Wang, P. Carbon-Layer-Protected Cuprous Oxide Nanowire Arrays for Efficient Water Reduction. *ACS Nano* **2013**, *7*, 1709−1717.
(96) Chen, Z. B.; Jaramillo, T. F.; Deutsch, T. G.; Kleiman-Shwarsctein, A.; Forman, A. J.; Gaillard, N.; Garland, R.; Takanabe, K.; Heske, C.; Sunkara, M.; McFarland, E. W.; Domen, K.; Miller, E. L.; Turner, J. A.; Dinh, H. N. Accelerating Materials Development for Photoelectrochemical Hydrogen Production: Standards for Methods, Definitions, and Reporting Protocols. *J. Mater. Res.* **2010**, *25*, 3−16.
(97) Neumann, B.; Bogdanoff, P.; Tributsch, H. TiO_2-Protected Photoelectrochemical Tandem Cu(In,Ga)Se_2 Thin Film Membrane for Light-Induced Water Splitting and Hydrogen Evolution. *J. Phys. Chem. C* **2009**, *113*, 20980−20989.
(98) Stavrides, A. Use of Amorphous Silicon Tandem Junction Solar Cells for Hydrogen Production in a Photoelectrochemical Cell. *Proc. SPIE* **2006**, *6340*, 63400K.
(99) Miller, E.; Rocheleau, R. E.; Khan, S. U. M. A Hybrid Multijunction Photoelectrode for Hydrogen Production Fabricated with Amorphous Silicon/Germanium and Iron Oxide Thin Films. *Int. J. Hydrogen Energy* **2004**, *29*, 907−914.

(100) van de Krol, R.; Liang, Y. An n-Si/n-Fe_2O_3 Heterojunction Tandem Photoanode for Solar Water Splitting. *Chimia* **2013**, *67*, 168−171.
(101) O'Regan, B.; Gratzel, M. A Low-Cost, High-Efficiency Solar Cell Based on Dye-Sensitized Colloidal TiO_2 Films. *Nature* **1991**, *353*, 737−740.
(102) Gratzel, M. Photoelectrochemical Cells. *Nature* **2001**, *414*, 338−344.
(103) Salvador, P.; Hidalgo, M. G.; Zaban, A.; Bisquert, J. Illumination Intensity Dependence of the Photovoltage in Nanostructured TiO_2 Dye-Sensitized Solar Cells. *J. Phys. Chem. B* **2005**, *109*, 15915−15926.
(104) Augustynski, J.; Calzaferri, G.; Courvoisier, J. C.; Gratzel, M. In *Hydrogen Energy Progress XI: Proceedings of the 11th World Hydrogen Energy Conference*, Stuttgart, Germany, **1996**, *3*, 2379−2387.
(105) Gratzel, M. The Artificial Leaf, Bio-Mimetic Photocatalysis. *CATTECH* **1999**, *3*, 3−17.
(106) Park, J. H.; Bard, A. J. Photoelectrochemical Tandem Cell with Bipolar Dye-Sensitized Electrodes for Vectorial Electron Transfer for Water Splitting. *Electrochem. Solid-State Lett.* **2006**, *9*, E5−E8.
(107) Arakawa, H.; Shiraishi, C.; Tatemoto, M.; Kishida, H.; Usui, D.; Suma, A.; Takamisawa, A.; Yamaguchi, T. Solar Hydrogen Production by Tandem Cell System Composed of Metal Oxide Semiconductor Film Photoelectrode and Dye-Sensitized Solar Cell. *Solar Hydrogen and Nanotechnology II* **2007**, *6650*, 65003−65003.
(108) Nazeeruddin, M. K.; Péchy, P.; Renouard, T.; Zakeeruddin, S. M.; Humphry-Baker, R.; Cointe, P.; Liska, P.; Cevey, L.; Costa, E.; Shklover, V.; Spiccia, L.; Deacon, G. B.; Bignozzi, C. A.; Grätzel, M. Engineering of Efficient Panchromatic Sensitizers for Nanocrystalline TiO_2-Based Solar Cells. *J. Am. Chem. Soc.* **2001**, *123*, 1613−1624.
(109) Yum, J. H.; Walter, P.; Huber, S.; Rentsch, D.; Geiger, T.; Nuesch, F.; De Angelis, F.; Gratzel, M.; Nazeeruddin, M. K. Efficient Far Red Sensitization of Nanocrystalline TiO_2 Films by an Unsymmetrical Squaraine Dye. *J. Am. Chem. Soc.* **2007**, *129*, 10320−10321.
(110) Shi, Y.; Hill, R. B. M.; Yum, J.-H.; Dualeh, A.; Barlow, S.; Grätzel, M.; Marder, S. R.; Nazeeruddin, M. K. A High-Efficiency Panchromatic Squaraine Sensitizer for Dye-Sensitized Solar Cells. *Angew. Chem.* **2011**, *123*, 6749−6751.
(111) Brillet, J.; Cornuz, M.; Le Formal, F.; Yum, J. H.; Graetzel, M.; Sivula, K. Examining Architectures of Photoanode-Photovoltaic Tandem Cells for Solar Water Splitting. *J. Mater. Res.* **2010**, *25*, 17−24.
(112) Yum, J.-H.; Baranoff, E.; Kessler, F.; Moehl, T.; Ahmad, S.; Bessho, T.; Marchioro, A.; Ghadiri, E.; Moser, J.-E.; Yi, C.; Nazeeruddin, M. K.; Grätzel, M. A Cobalt Complex Redox Shuttle for Dye-Sensitized Solar Cells with High Open-Circuit Potentials. *Nat. Commun.* **2012**, *3*, 631.
(113) Brillet, J.; Yum, J. H.; Cornuz, M.; Hisatomi, T.; Solarska, R.; Augustynski, J.; Graetzel, M.; Sivula, K. Highly Efficient Water Splitting by a Dual-Absorber Tandem Cell. *Nat. Photonics* **2012**, *6*, 824−828.
(114) Delcamp, J. H.; Yella, A.; Holcombe, T. W.; Nazeeruddin, M. K.; Grätzel, M. The Molecular Engineering of Organic Sensitizers for Solar-Cell Applications. *Angew. Chem., Int. Ed.* **2013**, *52*, 376−380.